fractal and fractional

MDPI

Article

Finite-Time Synchronization of Discontinuous Fractional-Order Multi-Layer Coupled Neural Networks via Aperiodic Intermittent Control

Bibo Zheng, Yunqiu Xu and Wei Dai *

School of Information and Control Engineering, China University of Mining and Technology, Xuzhou 221116, China; zhengbb@cumt.edu.cn (B.Z.); ts25060093a31tm@cumt.edu.cn (Y.X.)
* Correspondence: weidai@cumt.edu.cn

Abstract

This paper is mainly concentrated on finite-time synchronization (FTS) for discontinuous fractional-order multi-layer coupled neural networks (FMCNNs) under aperiodic intermittent control. The discontinuous activation function is introduced to capture abrupt transitions and switching phenomena widely observed in practical neural dynamics. However, such nonsmooth behaviors significantly increase the complexity of controller design and synchronization analysis. To cope with these problems, an aperiodic intermittent controller with a simple structure is developed within the Filippov differential inclusion framework, ensuring effective handling of nonsmooth neural dynamics while reducing control cost. More importantly, a piecewise fractional-order differential inequality is established to characterize the evolution of the Lyapunov function over the control and rest intervals under aperiodic switching. This inequality serves as a fundamental analytical tool for deriving sufficient conditions for FTS and estimating the settling time. Compared with the existing results, the proposed framework relaxes the restrictions on the power exponent and provides a more general analytical tool for investigating the FTS of discontinuous FMLCNNs. In the end, a simulation example is provided to show the validity of the proposed method.

Keywords: fractional-order multi-layer coupled neural networks; finite-time synchronization; discontinuous activation functions; aperiodic intermittent control

1. Introduction

Over the past few decades, coupled neural networks (CNNs) have been extensively studied due to their wide applications in various aspects, including biological neural systems [1], secure communication [2], power systems [3], and so on. In practice, many real-world systems, including social networks, transportation networks, and low-altitude economy systems, exhibit intrinsically multi-layer and cross-coupled characteristics [4–6]. Nevertheless, traditional single-layer CNNs are typically restricted to modeling a single type of coupling or homogeneous structures. To further capture these complex multi-coupling relationships, the framework of multi-layer coupled neural networks (MLCNNs) has been developed recently [7]. As a fundamental dynamic behavior, synchronization in CNNs is crucial for understanding information transmission and enhancing the coordination and adaptability of neural systems. This phenomenon essentially refers to the process in which CNNs nodes tend to reach a consistent and coordinated state under internal

Check for updates

Academic Editor: Ruihong Li

Received: 24 September 2026
Revised: 27 October 2026
Accepted: 29 October 2026
Published: 30 October 2026

Copyright: © 2026 by the authors. Licensee MDPI, Basel, Switzerland. This article is an open access article distributed under the terms and conditions of the Creative Commons Attribution (CC BY) license.

coupling or external control. Through this mechanism, a fundamental basis is provided for various applications, such as collective intelligence, pattern recognition, and collaborative mission planning [8–10]. Recently, the study of synchronization in MLCNNs has gradually attracted increasing attention [11–13].

Most existing MLCNNs are formulated via integer-order differential equations, which primarily describe the transient dynamics of node states. With the advancement of fractional calculus, it has been demonstrated that complex neural systems with memory and hereditary characteristics can be more accurately modeled through fractional-order frameworks [14–16]. In recent years, synchronization of fractional-order coupled neural networks (FOCNNs) has received considerable attention, and various synchronization problems have been investigated under different control strategies. For example, exponential outer quasi-synchronization of delayed FOCNNs has been studied via impulsive control [17], while Mittag–Leffler synchronization of FOCNNs with mixed delays has been investigated using a unified analytical framework [18]. These studies demonstrate the growing interest in synchronization analysis of FOCNNs involving complex network dynamics. Building on these advances, increasing efforts have been devoted to explore fractional-order multi-layer coupled neural networks (FMLCNNs), where various types of synchronization, including bipartite, quasi and projective synchronization, have been widely investigated [19–22]. Among these synchronization types, asymptotic convergence has been primarily considered, implying that synchronization can be realized only in infinite time. In practical engineering systems, it is often desirable that synchronization be achieved with faster convergence. This has motivated increasing research on finite-time synchronization (FTS), in which the synchronization error converges to zero within a finite settling time, offering fast convergence, strong robustness, and good disturbance rejection performance. Accordingly, a series of valuable findings on FTS of FMLCNNs have emerged in recent years [23–25]. However, these studies are conducted under the assumption that activation functions are continuous and satisfy the Lipschitz condition, which facilitates theoretical analysis. In many practical scenarios, neural systems exhibit switching behaviors and threshold effects, which prompts the use of discontinuous activation functions. These discontinuities give rise to complex analytical challenges, making the study of the FTS of FMLCNN with discontinuous activation functions of great theoretical significance.

Furthermore, continuous control schemes are utilized by most existing FTS strategies for FMLCNNs. Although rapid convergence can be ensured by such schemes, it inevitably leads to high energy consumption, excessive communication burden, and increased wear on actuators, which greatly limits its practical application, especially in large-scale or resource-constrained networks. To alleviate these issues, intermittent control, as an effective alternative, has been introduced, where the control input is activated only during specific time periods. In traditional intermittent control schemes, operations are typically conducted on a periodic manner, in which strictly pre-defined activation and rest intervals are required. In contrast, greater flexibility in controller scheduling is offered by aperiodic intermittent control, whereby the constraints of fixed activation patterns are removed, and a more suitable mechanism is provided for complex and uncertain environments [26,27]. To further clarify the differences among the existing studies, Table 1 provides a comparison of representative results.

Under the foregoing considerations, the FTS of FMLCNNs with discontinuous activation functions is addressed under aperiodic intermittent control. The main contributions are summarized as follows:

(1) Unlike most existing studies on MLCNNs that require the use of smooth activation functions or continuous control strategies [19,21–25], discontinuous activation functions

are considered in the proposed FMLCNNs under the Filippov differential inclusion framework, extending the synchronization analysis to discontinuous FMLCNNs.

(2) By exploring the aperiodic switching mechanism, a more general fractional-order differential inequality is developed, which improves the related results and provides a feasible method to investigate FTS of FMLCNNs.

(3) Compared with continuous control [23–25], a simple-structure non-periodic intermittent controller is designed, which effectively reduces the control cost while ensuring the FTS of considered FMLCNNs.

Table 1. Comparison of Existing Studies and the Proposed Work.

Content	**[20]**	**[21]**	**[22]**	**[25]**	**Proposed Work**
System model	Multi-weighted FOCNNs	Fractional-Order Fuzzy Multiplex Networks	Multi-weighted FOCNNs	FMLCNNs	FMLCNNs
Control strategy	Aperiodic intermittent control	Event-triggered control	Feedback control	Finite-time control	Finite-time aperiodic intermittent control
Discontinuous activation function	✓	–	–	–	✓
Finite-time convergence	–	–	–	✓	✓

The arrangement for the remainder of this paper is organized as follows. Section 2 presents the system model and preliminaries, including the necessary definitions and lemmas. Section 3 presents the main results on aperiodic intermittent control design and FTS of discontinuous FMLCNNs. In Section 4, a numerical example is shown to demonstrate the effectiveness of the theoretical results. Section 5 concludes the paper.

Notation 1. *Let* $\overrightarrow{\mathcal{N}} = \{1,2,\ldots,N\}$, $\overrightarrow{n} = \{1,2,\ldots,n\}$. *Let* $\mathbb{R}$ *be the set of real numbers and* $\mathbb{R}^l$ *denote a space with all l-dimensional real vectors.* $\mathbb{R}^{l\times l}$ *represents the set consisting of* $l \times l$ *real matrices.* $\mathbb{R}^+$ *denotes the set of positive constants.* $\mathbf{0}_l$ *is a l-dimensional full* 0 *column vector.* $\mathbb{I}_l$ *is an* $l-$*dimensional unit matrix. For real matrix* $\mathfrak{M}$, $\lambda_{\min}(\mathfrak{M})$ *and* $\lambda_{\max}(\mathfrak{M})$ *are the smallest and largest eigenvalues of* $\mathfrak{M}$, *respectively. For any* $z \in \mathbb{R}^n$, z^T *denotes its transpose and* $||z||_1 = \sum_{k=1}^{N} |z_k|$. $\mathbf{sign}(z) = (sign(z_1), sign(z_2), \ldots, sign(z_n))^T$ *and* $sgn^\theta(z) = (sign(z_1)|z_1|^\theta, \ldots, sign(z_n)|z_n|^\theta)^T$, *in which sign is a signum function.*

2. System Formulation and Preliminaries

2.1. System Description

Consider the following discontinuous FOCNNs with M-layer, in which each layer consists of N nodes:

$$\begin{aligned} {}_{t_0}^{C}\mathcal{D}_t^{\beta} y_k(t) = &- A y_k(t) + B g(y_k(t)) + J \\ &+ \sum_{l=1}^{M}\sum_{m=1}^{N} c^l h_{km}^l \Lambda^l y_m(t) + u_k(t),\ k \in \overrightarrow{\mathcal{N}} \end{aligned} \tag{1}$$

where $\beta \in (0,1)$, $y_k(t) = (y_{k1}(t), y_{k2}(t), \cdots, y_{kn}(t))^T \in \mathbb{R}^n$ is the state vector, $A = \mathrm{diag}\{a_1, \cdots, a_n\}$ denotes the self-feedback matrix with $a_i > 0$, $i \in \overrightarrow{n}$, $B \in \mathbb{R}^{n\times n}$ sig-

nifies connection weight matrix, $u_k(t) \in \mathbb{R}^n$ represents the control input, $c^l > 0$ is coupling strength of $l-$th layer, $g(y_k(t) = (g_1(y_k(t), \cdots, g_n(y_k(t))^T \in \mathbb{R}^n$ indicates the discontinuous activation function vector, Λ^l means the internal coupling matrix of the $l-$th layer, and the outer coupling matrix of the $l-$th layer is given as $H^l = (h^l_{km})_{N\times N}$, which satisfies $h^l_{kk} = -\sum\limits_{m=1,m\neq k}^{N} h^l_{km}$. Additionally, H^l is asymmetric, satisfying $h^l_{km} > 0$ if the node m and node k are connected $(m \neq k)$; otherwise, $h^l_{km} = 0, k, m \in \overrightarrow{\mathcal{N}}$. The initial condition of (1) is given as $y_k(t_0) = y_{k0}$, and the discontinuous activation functions $g_i(y_k(t), i \in \overrightarrow{n}$ are assumed to meet the following assumptions.

Assumption 1. *For $q \in \overrightarrow{n}$, $g_q(\cdot)$ is continuous except a countable set of isolate points $\{\varrho^q_k\}$. There exist finite left and right limits $g^-_q(\varrho^q_k)$, $g^+_q(\varrho^q_k)$. In addition, it has at most finite jump discontinuous on any compact interval.*

Assumption 2. *For $q \in \overrightarrow{n}$, $0 \in \mathbb{K}[g_q(0)]$, there exist constants $P > 0$, $Q > 0$ such that*

$$||\pi - \eta||_1 \leq P||a - b||_1 + Q,$$

in which $\pi \in \mathbb{K}[g_q(a)]$, $\eta \in \mathbb{K}[g_q(b)]$, $a \in \mathbb{R}^n$, $b \in \mathbb{R}^n$ and $\mathbb{K}[g_q(\cdot)] = [\min\{g^-_q(\cdot), g^+_q(\cdot)\}$, $\max\{g^-_q(\cdot), g^+_q(\cdot)\}]$, $\mathbb{K}[\cdot]$ denote the closure of the convex hull.

The dynamic behavior of the synchronization target $x(t)$ is given as

$$_{t_0}^{C}\mathcal{D}^{\beta}_t x(t) = -Ax(t) + Bg(x(t)) + J. \tag{2}$$

2.2. Preliminaries

Definition 1 ([28]). *A set-valued map is defined as*

$$\mathbb{K}[g](y(t)) = \bigcap_{\xi>0}\bigcap_{\mu(M)=0} \overline{co}\{g(B(y,\xi)) \setminus M\},$$

in which $\overline{co}$ is the convex closure. $\mu(M)$ indicates the Lebesgue measure of set M, $B(y,\xi) = \{x : ||x - y|| \leq \xi\}$.

Definition 2 ([14]). *For $\gamma, \beta > 0$, the definition of Mittag–Leffler function is defined by*

$$E_{\beta,\gamma}(y) = \sum_{k=0}^{\infty} \frac{y^k}{\Gamma(\beta k + \gamma)},$$

$$E_{\beta,1}(y) = E_{\beta}(y) = \sum_{k=0}^{\infty} \frac{y^k}{\Gamma(\beta k + 1)}.$$

Definition 3 ([14]). *The fractional-order integral of integrable function $y(t)$ with the order $\beta > 0$ is defined as*

$$_{t_0}I^{\beta}_t y(t) = \frac{1}{\Gamma(\beta)} \int_{t_0}^{t} (t-\rho)^{\beta-1} y(\rho) d\rho,$$

where

$$\Gamma(\beta) = \int_0^{\infty} e^{-t} t^{\beta-1} dt.$$

Definition 4 ([14]). *The Caputo fractional-order derivative of differentiable function $y(t)$ of order $\beta \in (0,1)$ is defined as*

$$_{t_0}^{C}\mathcal{D}^{\beta}_t y(t) = \frac{1}{\Gamma(1-\beta)} \int_{t_0}^{t} \frac{y'(\rho)}{(t-\rho)^{\rho}} d\rho.$$

Lemma 1 ([29]). *If continuous function* $\Psi(t) : [0, +\infty) \to \mathbb{R}^+$ *is differentiable and satisfies*

$$_0^C\mathcal{D}_t^\beta \Psi(t) \leq \alpha_1 \Psi(t) + \alpha_2, \quad t \geq t_0,$$

where $0 < \beta < 1$, $\alpha_1 > 0$, $\alpha_2 > 0$, *then*

$$\Psi(t) \leq \big(\Psi(t_0) + \frac{\alpha_2}{\alpha_1}\big) E_\beta(\alpha_1 (t - t_0)^\beta) - \frac{\alpha_2}{\alpha_1}.$$

Lemma 2 ([30]). *For* $\gamma \in \mathbb{R}^+$, *one has*

$$\Gamma(1 + \gamma) = \gamma \Gamma(\gamma).$$

Lemma 3 ([30]). *For any* $\gamma \in (0, 1)$ *and* $k \in \mathbb{N}^+$, *it has*

$$\big(\Gamma(1 + \gamma)\big)^k \leq \Gamma(1 + k\gamma) \leq k! \big(\Gamma(1 + \gamma)\big)^k.$$

In cases where the functions are not continuous or differentiable everywhere, such as discontinuous functions or absolute-value functions, it is considered to use the generalized Caputo fractional-order derivative to handle these special functions. For this purpose, the following lemmas are introduced:

Lemma 4 ([31]). *The generalized Caputo fractional-order derivative of* $y(t)$ *is defined as*

$$_{t_0}^C\mathcal{D}_t^{\beta^+} y(t) = \frac{1}{\Gamma(1 - \beta)} \int_{t_0}^t \frac{\mathcal{D}^+ y(\tau)}{(t - \tau)^\beta} d\tau, \quad 0 < \beta < 1,$$

in which $\mathcal{D}^+ y(t) = \limsup_{s \to 0^+} \dfrac{y(t + s) - y(t)}{s}$ *represents the upper right-hand Dini derivative of* $y(t)$.

Lemma 5 ([32]). *If* $y(t) : [t_0, +\infty) \to \mathbb{R}$ *is continuous, then for any* $\beta \in (0, 1)$,

$$_{t_0}^C\mathcal{D}_t^{\beta^+} |y(t)| \leq sign(y(t)) \, _{t_0}^C\mathcal{D}_t^\beta y(t), \ t \geq t_0.$$

Definition 5 ([33]). *The FOCNNs* (1) *are called to reach finite-time synchronization with system* (2) *if there exists a* $0 \leq T^*(e(t_0)) < +\infty$, *satisfying*

$$\lim_{t \to T^*(e(t_0))} ||e(t)|| = 0$$

and $||e(t)|| = 0$ *for* $t \geq T^*(e(t_0))$. *The settling time*

$$\begin{aligned} &T(e(t_0)) \\ &= \inf\{T^*(e(t_0)) \geq t_0 : ||e(t)|| = 0 \ \textit{for} \ \ t \geq T^*(e(t_0))\}, \end{aligned}$$

in which $e(t) = (e_1^T(t), \ldots, e_N^T(t))^T$ *and* $e_k(t) = z_k(t) - s(t)$, $k \in \mathcal{N}$.

3. Main Results

3.1. Aperiodic Intermittent Control Scheme

First, define the synchronization error $\omega_k(t) = y_k(t) - x(t)$. The intermittent control scheme is designed as

$$u_k(t) = \begin{cases} -d_k\omega_k(t) - \alpha \text{sign}(\omega_k(t)) \\ -\zeta_1 \text{sign}(\omega_k(t))\|\omega_k(t)\|_1^{\delta}, & t_i < t \le \theta_i, \\ 0, & \theta_i < t \le t_{i+1}, \end{cases} \tag{3}$$

where $\delta \in (0,1)$, $i \in \bar{\mathcal{N}} = \{0,1,2,\cdots\}$, $0 = t_0 < \theta_0 < t_1 < \cdots < t_i < \theta_i < t_{i+1} < \cdots$, t_i and θ_i indicate the time instants for the beginning and the end of the lth control, $t_{i+1} - t_i$ denotes the ith control period, $\theta_i - t_i$ and $t_{i+1} - \theta_i$ are the ith control and non-control width, $d_k > 0$, $\alpha > 0$, $\zeta_1 > 0$.

Remark 1. *Recent studies have investigated synchronization of fractional-order neural networks using quantized sampled-data control. For example, ref. [15] proposed a quantized sampled-data control strategy to achieve FTS of fractional-order neural networks, whereas ref. [16] studied the synchronization of fractional-order competitive neural networks via quantized sampled-data control. Different from these studies, an aperiodic intermittent control strategy is adopted to investigate the FTS of discontinuous FMLCNNs. This strategy allows the control input to be applied during control intervals and removed during rest intervals, while the lengths of these intervals need not follow a fixed periodic pattern. In contrast to the aforementioned studies, this paper focuses on FTS of discontinuous FMLCNNs under aperiodic intermittent control.*

Assumption 3. *There exist constants $T_c > 0$ and $T_r > 0$ such that $\inf\limits_{i\in\bar{\mathcal{N}}}\{\theta_i - t_i\} = T_c$, $\sup\limits_{i\in\bar{\mathcal{N}}}\{t_{i+1} - \theta_i\} = T_r$, $\sup\limits_{i\in\bar{\mathcal{N}}}\{t_{i+1} - t_i\} = T$.*

3.2. A Piecewise Fractional-Order Differential Inequality

To analyze the FTS problem under the aperiodic intermittent control scheme (3), a piecewise fractional-order differential inequality is established in Lemma 6, which characterizes the evolution of the Lyapunov function over the control intervals and the rest intervals, and serves as a fundamental tool for analyzing Theorem 1.

Lemma 6. *Let continuous function $\Phi(t) \in \mathcal{C}^1([t_0, +\infty), \mathbb{R}^+)$ satisfy the following inequalities:*

$$\begin{cases} {}_{t_i}^{C}\mathcal{D}_t^{\beta^+}\Phi(t) \le -\zeta_1\Phi^{\delta}(t) - \zeta_2, & t_i < t \le \theta_i, \\ {}_{\theta_i}^{C}\mathcal{D}_t^{\beta^+}\Phi(t) \le \varepsilon_1\Phi(t) + \varepsilon_2, & \theta_i < t \le t_{i+1}, \end{cases} \tag{4}$$

where $0 < \delta < 1$, $i \in \bar{\mathcal{N}} = \{0,1,2,\cdots\}$, $\zeta_1, \zeta_2 \in \mathbb{R}^+$, $\varepsilon_1, \varepsilon_2 \in \mathbb{R}^+$. Denote $\tilde{\Phi} = \Phi^{\delta-1}(t_0)$, $\lambda = \frac{\zeta_2}{\zeta_1\tilde{\Phi}}$, $\gamma = \frac{\varepsilon_2}{\varepsilon_1}$, $\varphi = E_\beta(-\zeta_1\tilde{\Phi}T_c^{\beta})E_\beta(\varepsilon_1 T_r^{\beta})$, $\mu = \gamma - (\gamma - \lambda)E_\beta(\varepsilon_1 T_r^{\beta})$. If $0 < \varphi < 1$, $\lambda > \gamma$, then

$$\Phi(t) = \Lambda(\Phi(t_0) + \lambda)E_\beta\left(\frac{ln\varphi}{T}(t - t_0)^{\beta}\right) - \lambda,$$

in which $\Lambda = \frac{1}{\varphi}exp(\Gamma(1+\beta))$.

Proof. For $i \in \bar{\mathcal{N}}$, if $t_i < t \le \theta_i$, based on Lemma 1, one has

$$\Phi(t) \le \big(\Phi(t_i) + \lambda\big)E_\beta(-\zeta_1\tilde{\Phi}(t - t_i)^{\beta}) - \lambda. \tag{5}$$

When $\theta_i < t \leq t_{i+1}$, in view of Lemma 1,

$$\Phi(t) \leq \big(\Phi(\theta_i) + \gamma\big) E_\beta(\varepsilon_1 (t - \theta_i)^\beta) - \gamma. \tag{6}$$

From (5) and (6), when $t_0 < t \leq \theta_0$,

$$\Phi(t) \leq \big(\Phi(t_0) + \lambda\big) E_\beta(-\zeta_1 \tilde{\Phi}(t - t_0)^\beta) - \lambda,$$

and

$$\Phi(\theta_0) \leq \big(\Phi(t_0) + \lambda\big) E_\beta(-\zeta_1 \tilde{\Phi}(\theta_0 - t_0)^\beta) - \lambda.$$

When $\theta_0 < t \leq t_1$, we have

$$\begin{aligned}
\Phi(t) \leq & \big(\Phi(\theta_0) + \gamma\big) E_\beta(\varepsilon_1 (t - \theta_0)^\beta) - \gamma \\
\leq & \big(\Phi(t_0) + \lambda\big) E_\beta(-\zeta_1 \tilde{\Phi} T_c^\beta) E_\beta(\varepsilon_1 (t - \theta_0)^\beta) \\
& + (\gamma - \lambda) E_\beta(\varepsilon_1 (t - \theta_0)^\beta) - \gamma,
\end{aligned}$$

and

$$\begin{aligned}
\Phi(t_1) \leq & \big(\Phi(t_0) + \lambda\big) E_\beta(-\zeta_1 \tilde{\Phi} T_c^\beta) E_\beta(\varepsilon_1 (t_1 - \theta_0)^\beta) \\
& + (\gamma - \lambda) E_\beta(\varepsilon_1 (t_1 - \theta_0)^\beta) - \gamma \\
\leq & \big(\Phi(t_0) + \lambda\big) E_\beta(-\zeta_1 \tilde{\Phi} T_c^\beta) E_\beta(\varepsilon_1 T_r^\beta) \\
& + (\gamma - \lambda) E_\beta(\varepsilon_1 T_r^\beta) - \gamma \\
= & \big(\Phi(t_0) + \lambda\big) \varphi + (\gamma - \lambda) E_\beta(\varepsilon_1 T_r^\beta) - \gamma.
\end{aligned}$$

When $t_1 < t \leq \theta_1$,

$$\begin{aligned}
\Phi(t) \leq & \big(\Phi(t_1) + \lambda\big) E_\beta(-\zeta_1 \tilde{\Phi}(t - t_1)^\beta) - \lambda \\
\leq & \big(\Phi(t_0) + \lambda\big) \varphi E_\beta(-\zeta_1 \tilde{\Phi}(t - t_1)^\beta) \\
& + \lambda E_\beta(-\zeta_1 \tilde{\Phi}(t - t_1)^\beta) - \lambda \\
& + \big((\gamma - \lambda) E_\beta(\varepsilon_1 T_r^\beta) - \gamma\big) E_\beta(-\zeta_1 \tilde{\Phi}(t - t_1)^\beta),
\end{aligned}$$

and

$$\begin{aligned}
\Phi(\theta_1) \leq & \big((\gamma - \lambda) E_\beta(\varepsilon_1 T_r^\beta) - \gamma\big) E_\beta(-\zeta_1 \tilde{\Phi} T_c^\beta) \\
& + \big(\Phi(t_0) + \lambda\big) \varphi E_\beta(-\zeta_1 \tilde{\Phi} T_c^\beta) \\
& + \lambda E_\beta(-\zeta_1 \tilde{\Phi} T_c^\beta) - \lambda.
\end{aligned}$$

When $\theta_1 < t \leq t_2$,

$$\begin{aligned}
\Phi(t) \leq & \big(\Phi(\theta_1) + \gamma\big) E_\beta(\varepsilon_1 (t - \theta_1)^\beta) - \gamma \\
\leq & \Big(\big(\Phi(t_0) + \lambda\big) \varphi E_\beta(-\zeta_1 \tilde{\Phi} T_c^\beta) + \lambda E_\beta(-\zeta_1 \tilde{\Phi} T_c^\beta) \\
& + \big((\gamma - \lambda) E_\beta(\varepsilon_1 T_r^\beta) - \gamma\big) E_\beta(-\zeta_1 \tilde{\Phi} T_c^\beta)\Big) \\
& * E_\beta(\varepsilon_1 (t - \theta_1)^\beta) + (\gamma - \lambda) E_\beta(\varepsilon_1 (t - \theta_1)^\beta) - \gamma,
\end{aligned}$$

and

$$\begin{aligned}\Phi(t_2) \leq & \big(\Phi(t_0)+\lambda\big)\varphi^2+\lambda\varphi+\big((\gamma-\lambda)E_\beta(\varepsilon_1 T_r^\beta)-\gamma\big)\varphi \\ & +(\gamma-\lambda)E_\beta(\varepsilon_1 T_r^\beta)-\gamma.\end{aligned}$$

When $t_2 < t \leq \theta_2$,

$$\begin{aligned}\Phi(t) \leq & \big(\Phi(t_2)+\lambda\big)E_\beta(-\zeta_1\tilde{\Phi}(t-t_2)^\beta)-\lambda \\ \leq & \big(\Phi(t_0)+\lambda\big)\varphi^2 E_\beta(-\zeta_1\tilde{\Phi}(t-t_2)^\beta) \\ & +\big(\lambda\varphi-\mu\varphi-\mu\big)E_\beta(-\zeta_1\tilde{\Phi}(t-t_2)^\beta) \\ & +\lambda E_\beta(-\zeta_1\tilde{\Phi}(t-t_2)^\beta)-\lambda,\end{aligned}$$

and

$$\begin{aligned}\Phi(\theta_2) \leq & \big(\Phi(t_0)+\lambda\big)\varphi^2 E_\beta(-\zeta_1\tilde{\Phi}T_c^\beta) \\ & +\big(\lambda\varphi-\mu\varphi-\mu\big)E_\beta(-\zeta_1\tilde{\Phi}T_c^\beta) \\ & +\lambda E_\beta(-\zeta_1\tilde{\Phi}T_c^\beta)-\lambda.\end{aligned}$$

Similarly, when $\theta_2 < t \leq t_3$,

$$\begin{aligned}\Phi(t) \leq & \big(\Phi(\theta_2)+\gamma\big)E_\beta(\varepsilon_1(t-\theta_2)^\beta)-\gamma \\ \leq & \Big(\big(\Phi(t_0)+\lambda\big)\varphi^2+(\lambda\varphi-\mu\varphi)-\mu\Big) \\ & *E_\beta(-\zeta_1\tilde{\Phi}T_c^\beta)E_\beta(\varepsilon_1(t-\theta_2)^\beta)-\gamma \\ & +\big(\lambda E_\beta(-\zeta_1\tilde{\Phi}T_c^\beta)-\lambda+\gamma\big)E_\beta(\varepsilon_1(t-\theta_2)^\beta), \\ \Phi(t_3) \leq & \big(\Phi(t_0)+\lambda\big)\varphi^3-\mu\varphi^2+\lambda\varphi^2-\mu\varphi+\lambda\varphi-\mu.\end{aligned}$$

According to the above analysis, it can be obtained by the iterative method:

$$\begin{cases}\Phi(t_i) \leq & \big(\Phi(t_0)+\lambda\big)\varphi^i+(\lambda-\mu)\frac{1-\varphi^i}{1-\varphi}-\lambda, \\ \Phi(\theta_i) \leq & \big[\big(\Phi(t_0)+\lambda\big)\varphi^i+(\lambda-\mu)\frac{1-\varphi^i}{1-\varphi}-\lambda\big] \\ & *E_\beta(-\zeta_1\tilde{\Phi}T_c^\beta)+\lambda E_\beta(-\zeta_1\tilde{\Phi}T_c^\beta)-\lambda.\end{cases} \tag{7}$$

By combining the inequality (5) and (7), and using the property of Mittag–Leffler function, we can get, for any $t_i < t \leq \theta_i$,

$$\begin{aligned}\Phi(t) \leq & \big[\big(\Phi(t_0)+\lambda\big)\varphi^i+\lambda\varphi^{i-1}+\lambda\varphi^{i-2}+\cdots+\lambda\varphi+\lambda \\ & -\mu\varphi^{i-1}-\mu\varphi^{i-2}-\cdots-\mu\big]E_\beta(-\zeta_1\tilde{\Phi}(t-t_i)^\beta)-\lambda \\ \leq & \big(\Phi(t_0)+\lambda\big)\varphi^i+(\lambda-\mu)\frac{1-\varphi^i}{1-\varphi}-\lambda.\end{aligned} \tag{8}$$

For any $\theta_i < t \leq t_{i+1}$, one has

$$\begin{aligned}\Phi(t) \leq & \big[\big(\Phi(t_0)+\lambda\big)\varphi^i+\lambda\varphi^{i-1}+\lambda\varphi^{i-2}+\cdots+\lambda\varphi \\ & +\lambda-\mu\varphi^{i-1}-\mu\varphi^{i-2}-\cdots-\mu\big] \\ & *E_\beta(-\zeta_1\tilde{\Phi}T_c^\beta)E_\beta(\varepsilon_1(t-\theta_i)^\beta) \\ & +(\gamma-\lambda)E_\beta(\varepsilon_1(t-\theta_i)^\beta)-\gamma \\ \leq & \big(\Phi(t_0)+\lambda\big)\varphi^i+(\lambda-\mu)\frac{1-\varphi^i}{1-\varphi}-\mu.\end{aligned} \tag{9}$$

From $0 < \varphi < 1$, $1 < \frac{1-\varphi^i}{1-\varphi} < \frac{1}{1-\varphi}$ can be derived. In addition, based on $\mu = \gamma - (\gamma - \lambda)E_\beta(\varepsilon_1 T_r^\beta)$, $\lambda > \gamma$ one has $\gamma - (\gamma - \lambda)E_\beta(\varepsilon_1 T_r^\beta) - \lambda > 0$. Then, $\mu > \lambda$.

Therefore, using Lemma 3 and combining (8)–(9), one gets

$$\begin{aligned}\Phi(t) \leq & \big(\Phi(t_0) + \lambda\big)\varphi^i + (\lambda - \mu)\frac{1-\varphi^i}{1-\varphi} - \lambda \\ \leq & \big(\Phi(t_0) + \lambda\big)\varphi^{\frac{t-t_0}{T}-1} - \lambda \\ \leq & \varphi^{-1}\big(\Phi(t_0) + \lambda\big)\exp\big(\frac{\ln\varphi}{T}(t-t_0)\big) - \lambda \\ \leq & \Lambda\big(\Phi(t_0) + \lambda\big)E_\beta\big(\ln\varphi\frac{(t-t_0)^\beta}{T}\big) - \lambda, \end{aligned} \tag{10}$$

in which $\Lambda = \frac{1}{\varphi}\exp(\Gamma(1+\beta))$.

Denote

$$Q(t) = \Lambda\big(\Phi(t_0) + \lambda\big)E_\beta\big(\ln\varphi\frac{(t-t_0)^\beta}{T}\big) - \lambda, \tag{11}$$

and in view of $\ln\varphi < 0$ and Lemma 2, function $E_\beta(\ln\varphi\frac{(t-t_0)^\beta}{T})$ is monotonically non-increasing and $0 < E_\beta(\ln\varphi\frac{(t-t_0)^\beta}{T}) < 1$. Hence, $Q(t)$ is also monotonically non-increasing.

Suppose there exists $\check{t} > t_0$ such that $Q(\check{t}) = 0$, and for any $t > \check{t}$, it holds that $Q(t) = 0$. Otherwise, there would exist $\hat{t} > \check{t}$ such that $Q(\hat{t}) > 0$. From (11), we know that

$$Q(\hat{t}) = \Lambda\big(\Phi(t_0) + \lambda\big)E_\beta\big(\ln\varphi\frac{(\hat{t}-t_0)^\beta}{T}\big) - \lambda \leq Q(\check{t}),$$

and hence, $Q(\hat{t}) \leq 0$. Clearly, this contradicts the assumption that $Q(\hat{t}) > 0$. Therefore, for all $t \geq \check{t}$, we have $\Phi(t) \leq Q(t) \leq 0$.

In the following, we prove the existence of $\check{t}$. When $\beta \in (0,1)$, according to the properties of the Mittag–Leffler function, it is known that $E_\beta(0) = 1$, and $\lim_{t\to+\infty} E_\beta(-t) = 0$. From this, we can deduce that $Q(t_0) > 0$, $\lim_{t\to+\infty} Q(t) < 0$, and $\lim_{t\to+\infty} Q(t) < 0$. Therefore, there must exist a $\check{t} > t$ such that $Q(\check{t}) = 0$ holds.

We then determine the time at which the upper bound reaches zero by solving $Q(\check{t}) = 0$. Taking $Q(\check{t}) = 0$ yields

$$E_\beta\big(\ln\varphi\frac{(\check{t}-t_0)^\beta}{T}\big) = \frac{\lambda}{\Lambda\big(\Phi(t_0) + \lambda\big)}.$$

Specifically, define $\nu = \max\{z \mid E_\beta(z) = \frac{\lambda}{\Lambda\left(\Phi(t_0)+\lambda\right)}\}$. By the definition of ν, we have

$$\ln\varphi\frac{(\check{t}-t_0)^\beta}{T} = \nu.$$

Solving for $\check{t}$ yields

$$\check{t} = t_0 + \left(\frac{\nu T}{\ln\varphi}\right)^{1/\beta}.$$

Based on the above analysis, the settling time T^* can be calculated as

$$T^* \leq \check{t} = t_0 + \left(\frac{\nu T}{\ln\varphi}\right)^{1/\beta}.$$

□

Remark 2. *Lemma 6 plays a fundamental role in this paper. It provides a unified analytical framework for characterizing the evolution of the Lyapunov function over the control and rest intervals under aperiodic intermittent control. The resulting piecewise fractional-order inequality is transformed into an explicit Mittag–Leffler-type bound, which facilitates the derivation of the finite settling time. In particular, compared with existing result in [27], a less restrictive condition on the power exponent is required, which the restriction is relaxed from* $0 < \gamma < \alpha < 1$ *to* $0 < \delta < 1$.

By applying Lemma 6 to the Lyapunov function associated with the synchronization error, the following FTS result can be obtained.

3.3. FTS Control for Discontinuous FMCNNs

Theorem 1. *Under Assumptions 1–3, the discontinuous FOCNNs (1) can be achieved FTS with intermittent control scheme (3) if diagonal matrix D exists and constants* ε_1, ε_2, ζ_1, ζ_2 *satisfy the following conditions:*

$$(\sigma P - a_q)\mathbb{E}_N - D + \sum_{l=1}^{M} c^l \gamma_q^l H^l \leq 0,\ \zeta_2 = \alpha - n\tilde{\sigma}NQ > 0,$$

$$\varepsilon_1 = \min_{1\leq q\leq n} \left(\lambda_{\min}((\sigma P - a_q)\mathbb{E}_N + \sum_{l=1}^{M} c^l \gamma_q^l H^l)\right) > 0,$$

$$\varphi = E_\beta(-\zeta_1 \tilde{V} T_c^\beta) E_\beta(\varepsilon_1 T_r^\beta) < 1,\ \ \lambda > \varepsilon_2/\varepsilon_1.$$

Furthermore, the settling-time $T^\diamond$ *is calculated as*

$$T^\diamond \leq \check{t} = t_0 + (\frac{\nu T}{ln\varphi})^{\frac{1}{\beta}},$$

where

$$\varepsilon_2 = n\tilde{\sigma}NQ,\ \ \lambda = \frac{\zeta_2}{\zeta_1 \tilde{V}},$$

$$\nu = \max\{z \mid E_\beta(z) = \frac{\lambda}{\Lambda\big(V(t_0) + \lambda\big)}\} < 0,$$

$$\tilde{V} = V^{\delta-1}(t_0),\ \Lambda = \frac{1}{\varphi} exp(\Gamma(1+\beta)),$$

$$\sigma = \max_{1\leq q\leq n}\{\sum_{\eta=1}^{n} |b_{\eta q}|\},\ \ \tilde{\sigma} = \max_{1\leq q\leq n}\{\sum_{\eta=1}^{n} |b_{q\eta}|\}.$$

Proof. Based on the control scheme (3), set-valued maps and differential inclusion theory [28,34] are adopted to solve FOCNNs (1) and (2). Then, from (1),

$$\begin{cases} {}_{t_i}^{C}\mathcal{D}_t^\beta y_k(t) \in & -Ay_k(t) + B\mathbb{K}[g(y_k(t))] + J - d_k\omega_k(t) \\ & + \sum_{l=1}^{M}\sum_{m=1}^{N} c^l h_{km}^l \Lambda^l y_m(t) - \alpha \mathrm{SIGN}(\omega_k(t)) \\ & -\zeta_1 \mathrm{sign}(\omega_k(t))\|\omega_k(t)\|_1^\delta, \quad t_i < t \leq \theta_i, \\ {}_{\theta_i}^{C}\mathcal{D}_t^\beta y_k(t) \in & -Ay_k(t) + B\mathbb{K}[g(y_k(t))] + J \\ & + \sum_{l=1}^{M}\sum_{m=1}^{N} c^l h_{km}^l \Lambda^l y_m(t), \quad \theta_i < t \leq t_{i+1}. \end{cases} \tag{12}$$

Similarly, from (2),

$${}_{t_0}^{C}\mathcal{D}_t^\beta x(t) \in -Ax(t) + B\mathbb{K}[g(x(t))] + J, \tag{13}$$

where

$$\mathbb{K}[g(y_k(t))] = (\mathbb{K}[g_1(y_k(t))], \cdots, \mathbb{K}[g_n(y_k(t))])^T,$$
$$\mathbb{K}[g(x(t))] = (\mathbb{K}[g_1(x(t))], \cdots, \mathbb{K}[g_n(x(t))])^T,$$
$$\mathrm{SIGN}(\omega_k(t)) = (\mathrm{SIGN}(\omega_{k1}(t)), \cdots, \mathrm{SIGN}(\omega_{kn}(t)))^T.$$

Furthermore, for any $1 \le k \le N$, $1 \le q \le n$,

$$\mathrm{SIGN}(\omega_{kq}(t)) = \begin{cases} \{-1\}, & \omega_{kq}(t) < 0, \\ [-1,1], & \omega_{kq}(t) = 0, \\ \{1\}, & \omega_{kq}(t) > 0. \end{cases}$$

By using the measurable selection theorem [28], one can find measurable functions such that $\pi_k(t) \in \mathbb{K}[g(z_k(t))]$, $\tilde{\pi}(t) \in \mathbb{K}[g(s(t))]$, $\varrho_k(t) \in \mathrm{SIGN}(\omega_k(t))$,

$$\begin{cases} {}_{t_i}^{C}\mathcal{D}_t^{\beta} y_k(t) = & -A y_k(t) + B\pi_k(t) + J - \alpha\varrho_k(t) \\ & + \sum_{l=1}^{M}\sum_{m=1}^{N} c^l h_{km}^l \Lambda^l y_m(t) - d_k\omega_k(t) \\ & -\zeta_1 \mathrm{sign}(\omega_k(t))\|\omega_k(t)\|_1^{\delta}, \ t_i < t \le \theta_i, \\ {}_{\theta_i}^{C}\mathcal{D}_t^{\beta} y_k(t) = & -A y_k(t) + B\pi_k(t) + J \\ & + \sum_{l=1}^{M}\sum_{m=1}^{N} c^l h_{km}^l \Lambda^l y_m(t), \ \theta_i < t \le t_{i+1}, \end{cases} \tag{14}$$

and

$${}_{t_0}^{C}\mathcal{D}_t^{\beta} x(t) = -Ax(t) + B\tilde{\pi}(t) + J. \tag{15}$$

Based on systems (14) and (15), the error system can be derived as

$$\begin{cases} {}_{t_i}^{C}\mathcal{D}_t^{\beta} \omega_k(t) = & -A\omega_k(t) + B\big(\pi_k(t) - \tilde{\pi}(t)\big) - d_k\omega_k(t) \\ & + \sum_{l=1}^{M}\sum_{m=1}^{N} c^l h_{km}^l \Lambda^l \omega_m(t) - \alpha\varrho_k(t) \\ & -\zeta_1 \mathrm{sign}(\omega_k(t))\|\omega_k(t)\|_1^{\delta}, \quad t_i < t \le \theta_i, \\ {}_{\theta_i}^{C}\mathcal{D}_t^{\beta} \omega_k(t) = & -A\omega_k(t) + B\big(\pi_k(t) - \tilde{\pi}(t)\big) \\ & + \sum_{l=1}^{M}\sum_{m=1}^{N} c^l h_{km}^l \Lambda^l \omega_m(t), \quad \theta_i < t \le t_{i+1}. \end{cases} \tag{16}$$

Next, consider the Lyapunov function:

$$V(t) = \sum_{k=1}^{N} ||\omega_k(t)||_1 = \sum_{k=1}^{N}\sum_{q=1}^{n} |\omega_{kq}(t)|.$$

When $t \in (t_i, \theta_i]$, form Lemma 5, one has

$$\begin{aligned} & {}_{t_i}^{C}\mathcal{D}_t^{\beta^+} V(t) \\ & \le \sum_{k=1}^{N} \mathrm{sign}^T(\omega_k(t)) \, {}_{t_0}^{C}\mathcal{D}_t^{\beta} \omega_k(t) \\ & = \sum_{k=1}^{N} \mathrm{sign}^T(\omega_k(t)) \Big(-A\omega_k(t) + B\big(\pi_k(t) - \tilde{\pi}(t)\big) \\ & \quad + \sum_{l=1}^{M}\sum_{m=1}^{N} c^l h_{km}^l \Lambda^l \omega_m(t) - \alpha\varrho_k(t) - d_k\omega_k(t) \\ & \quad - \zeta_1 \mathrm{sign}(\omega_k(t))\|\omega_k(t)\|_1^{\delta} \Big). \end{aligned} \tag{17}$$

Since $h_{km} > 0 (k \neq m)$ and Γ is a positive definite diagonal matrix,

$$\begin{aligned}
&\sum_{k=1}^{N}\sum_{l=1}^{M}\sum_{m=1}^{N} \operatorname{sign}^T(\omega_k(t)) c^l h_{km}^l \Lambda^l \omega_m(t) \\
=&\sum_{k=1}^{N}\sum_{l=1}^{M}\sum_{m=1}^{N}\sum_{q=1}^{n} \operatorname{sign}(\omega_{kq}(t)) c^l h_{km}^l \gamma_q^l \omega_{mq}(t) \\
\leq&\sum_{l=1}^{M}\sum_{q=1}^{n} c^l \gamma_q^l \Big(\sum_{k=1}^{N} h_{kk}^l |\omega_{kq}(t)| + \sum_{k=1}^{N}\sum_{m=1,m\neq k}^{N} h_{km}^l |\omega_{mq}(t)| \Big) \\
=&\sum_{l=1}^{M}\sum_{q=1}^{n} c^l \gamma_q^l \mathbf{1}_N^T H^l \hat{\omega}_q(t),
\end{aligned} \tag{18}$$

in which $\hat{\omega}_q(t) = \big(|\omega_{1q}(t)|_1, \cdots, |\omega_{Nq}(t)|_1\big)^T$.

According to Assumption 2, we have

$$\begin{aligned}
&\sum_{k=1}^{N} \operatorname{sign}^T(\omega_k(t)) B\big(\pi_k(t) - \tilde{\pi}(t)\big) \\
=&\sum_{k=1}^{N}\sum_{q=1}^{n}\sum_{\eta=1}^{n} \operatorname{sign}(\omega_{kq}(t)) b_{i\eta} \big(\pi_{k\eta}(t) - \tilde{\pi}_\eta(t)\big) \\
=&\sum_{k=1}^{N}\sum_{q=1}^{n}\sum_{\eta=1}^{n} |b_{q\eta}| |\big(\pi_{k\eta}(t) - \tilde{\pi}_\eta(t)\big)| \\
\leq& P \sum_{k=1}^{N}\sum_{q=1}^{n}\sum_{\eta=1}^{n} |b_{\eta q}| |\omega_{kq}(t)| + NQ \sum_{q=1}^{n}\sum_{\eta=1}^{n} |b_{q\eta}| \\
\leq& \sigma P \sum_{q=1}^{n} |\omega_q(t)| + n\tilde{\sigma} NQ,
\end{aligned} \tag{19}$$

where $\sigma = \max\limits_{1\leq q\leq n} \{ \sum\limits_{\eta=1}^{n} |b_{\eta q}| \}$, $\tilde{\sigma} = \max\limits_{1\leq q\leq n} \{ \sum\limits_{\eta=1}^{n} |b_{q\eta}| \}$.

Substituting inequalities (18) and (19) into (17), when $t \in (t_i, \theta_i]$, we have

$$\begin{aligned}
&{}_{t_i}^{C}\mathcal{D}_t^{\beta^+} V(t) \\
\leq&\sum_{k=1}^{N}\sum_{q=1}^{n} (\sigma P - a_q - d_k) |\omega_{kq}(t)| + n\tilde{\sigma} NQ - \alpha \\
&+ \sum_{l=1}^{M}\sum_{q=1}^{n} c^l \gamma_q^l \mathbf{1}_N^T H^l \hat{\omega}_q(t) - \zeta_1 \sum_{k=1}^{N}\sum_{q=1}^{n} |\omega_{kq}(t)|^\delta \\
=&\sum_{q=1}^{n} \mathbf{1}_N^T \big((\sigma P - a_q) \mathbb{E}_N - D + \sum_{l=1}^{M} c^l \gamma_q^l H^l \big) \hat{\omega}_q(t) \\
&+ n\tilde{\sigma} NQ - \alpha - \zeta_1 \sum_{k=1}^{N}\sum_{q=1}^{n} |\omega_{kq}(t)|^\delta \\
\leq& -\zeta_1 \sum_{k=1}^{N}\sum_{q=1}^{n} |\omega_{kq}(t)|^\delta - \zeta_2,
\end{aligned} \tag{20}$$

in which $D = \operatorname{diag}(d_1, d_2, \cdots, d_N)$.

Because $\delta \in (0,1)$, one has

$$\sum_{k=1}^{N}\sum_{q=1}^{n}|\omega_{kq}(t)|^{\delta} \geq V^{\delta}(t),$$

then

$$\overset{C}{t_0}\mathcal{D}_t^{\beta^+}V(t) \leq -\zeta_1 V^{\delta}(t) - \zeta_2, \ \ t \in (t_i, \theta_i]. \tag{21}$$

Similarly, when $t \in (\theta_i, t_{i+1}]$, one gets

$$\begin{aligned}
&\overset{C}{\theta_i}\mathcal{D}_t^{\beta^+}V(t)\\
&\leq \sum_{q=1}^{n}\mathbf{1}_N^T\big((\sigma P - a_q)\mathbb{E}_N + \sum_{l=1}^{M}c^l\gamma_q^l H^l\big)\hat{\omega}_q(t) + n\tilde{\sigma}NQ\\
&=\varepsilon_1 V(t) + \varepsilon_2.
\end{aligned} \tag{22}$$

Then, combining inequalities (21) and (22), and based on Lemma 6, one has

$$V(t) = \Lambda(V(t_0)+\lambda)E_{\beta}(\frac{ln\varphi}{T}(t-t_0)^{\beta}) - \lambda,$$

where $\Lambda = \frac{1}{\varphi}\exp(\Gamma(1+\beta))$, $\lambda = \frac{\zeta_2}{\zeta_1 V^{\delta-1}(t_0)}$, $\varphi = E_{\beta}(-\zeta_1\tilde{V}T_c^{\beta})E_{\beta}(\varepsilon_1 T_r^{\beta}) < 1$, $\tilde{V} = V^{\delta-1}(t_0)$.

Before applying Lemma 6, we clarify how the conditions in Theorem 1 are related to the assumptions of this lemma. In particular, the condition $\zeta_2 = \alpha - n\tilde{\sigma}NQ > 0$, together with the positivity of ζ_1 and $\tilde{V}$, ensures that $\lambda = \zeta_2/(\zeta_1\tilde{V}) > 0$. $\lambda > \varepsilon_2/\varepsilon_1$ is equivalent to $\varepsilon_1\zeta_2 > \varepsilon_2\zeta_1\tilde{V}$, provided that ζ_1, $\tilde{V}$, and ε_1 are positive. Furthermore, the condition $\varphi < 1$ is essential for establishing the Mittag–Leffler-type bound and deriving the settling-time estimate. Once all the required conditions are verified, Lemma 6 can be directly applied to the derived fractional-order differential inequality for the Lyapunov function, yielding the FTS result and the corresponding settling-time bound.

Furthermore, following a similar procedure to that in the proof of Lemma 6, the settling-time bound can be obtained as

$$T^{\diamond} \leq \check{t} = t_0 + (\frac{\nu T}{\ln\varphi})^{\frac{1}{\beta}}.$$

Then, for any $t \geq T^{\diamond}$, $V(t) = 0$ holds, which means when $t \geq T^{\diamond}$, $\| \omega(t) \| = 0$ and FOCNNs (1) can be realized FTS under control scheme (3). □

Remark 3. *Different from existing studies on MLCNNs that mainly consider smooth activation functions or continuous control strategies [19,21–25], this paper investigates the FTS of FMLCNNs with discontinuous activation functions. In the proof of Theorem 1, the discontinuous neural dynamics are reformulated as a Filippov differential inclusion, providing a rigorous framework for analyzing the resulting nonsmooth system. Moreover, under the aperiodic switching mechanism, a more general fractional-order differential inequality, is established to derive sufficient conditions for FTS. These results extend the existing synchronization analysis of MLCNNs to discontinuous fractional-order multi-layer networks under aperiodic intermittent control.*

Remark 4. *It is worth noting that the sign function used in controller (3) may cause chattering in practical applications.A possible approach to address this issue is to replace the sign function with a smooth approximation, such as the hyperbolic tangent function or saturation function. Although a saturation-function-based control strategy has been investigated for FTS in [35], extending such*

an approach to the present FMLCNNs remains challenging. Specifically, the approximation error introduced by replacing the discontinuous sign function may affect the key inequalities in the Lyapunov-based stability analysis, making it difficult to establish sufficient conditions for FTS under the modified controller. In particular, whether exact FTS can be preserved or only convergence to a small neighborhood of the synchronization manifold can be guaranteed remains to be investigated in future work.

Remark 5. *Interconnected fractional-order neural circuits provide a potential application of the considered framework. For example, an analog circuit for a fractional-order Hopfield neural network was designed and simulated in [36]. In a circuit interpretation of the considered model, the node states represent neuron voltages, and the coupling layers describe different interconnection channels. The synchronization objective is to make the corresponding voltages follow those of a reference circuit with corrective inputs applied during the working intervals of the aperiodic intermittent controller. This circuit interpretation suggests a potential application of the proposed synchronization method, while its implementation and validation in a specific circuit require further investigation.*

4. Numerical Simulations

In this section, we show a simulation example to verify the effectiveness of proposed aperiodic intermittent control scheme. First, consider the following FMLCNNs with five nodes:

$$\begin{aligned} {}_{t_0}^{C}\mathcal{D}_t^{\beta} y_k(t) =& -Ay_k(t) + Bg(y_k(t)) + J \\ &+ \sum_{l=1}^{3}\sum_{m=1}^{5} c^l h_{km}^l \Lambda^l y_m(t) + u_k(t), \quad k = 1, \cdots, 5, \end{aligned} \tag{23}$$

where

$$A = \begin{bmatrix} 1 & 0 & 0 \\ 0 & 1 & 0 \\ 0 & 0 & 1 \end{bmatrix}, \quad B = \begin{bmatrix} 1.8 & -1.15 & -0.05 \\ 1.79 & 1.41 & 1.14 \\ -3.45 & 0 & 1 \end{bmatrix},$$

and $y_k(t) = (y_{k1}(t), y_{k2}(t), y_{k3}(t))^T$, $\beta = 0.98$, $c^l = 0.1$, $\Lambda^l = \mathbb{E}_3$, $g(y_k) = (g_1(y_{k1}), g_2(y_{k2}), g_3(y_{k3}))^T$ satisfies

$$g_q(y_{kq}) = \begin{cases} 0.5\tanh(y_{kq}) - 0.01, & y_{kq} > 0, \\ 0.5\tanh(y_{kq}) + 0.01, & y_{kq} \leq 0, \end{cases}$$

where $q = 1, 2, 3$.

The network structure of FOCNNs (23) are depicted in Figure 1.

The dynamical behavior of the 3-dimensional target system $x(t)$ is presented as follows:

$${}_{t_0}^{C}\mathcal{D}_t^{\beta} x(t) = -Ax(t) + Bg(x(t)) + J. \tag{24}$$

System (24) initialized with $x_1(0) = 0.2, x_2(0) = -0.2, x_3(0) = 0.2$ exhibits a chaotic attractor, as depicted in Figure 2.

Select $d_k = 2.83$, $\alpha = 7.67$, $\delta = 0.8$, $\zeta_1 = 3$; then, the controller is

$$u_k(t) = \begin{cases} -2.83\omega_k(t) - 7.67\text{sign}(\omega_k(t)) & \\ -3\text{sign}(\omega_k(t))\|\omega_k(t)\|_1^{0.8}, & t_i < t \leq \theta_i, \\ 0, & \theta_i < t \leq t_{i+1}, \end{cases} \tag{25}$$

where $i \in \mathcal{N}$. By simple calculation, it is obvious that $P = 0.5$, $Q = 0.02$, $V(t_0) = 12.1$, $\sigma = 7.04$ and $\tilde{\sigma} = 4.45$. Choose $\varepsilon_1 = 1.3663$, $\varepsilon_2 = 1.335$, $T_c = 1.2$, $T_r = 0.6$, T = 1.8,

$\varphi = 0.2770$, $\ln\varphi = -1.2836$, $\zeta_2 = 6.335$, $\lambda = 3.4768$, $\gamma = 0.9771$, $\nu = -4.1294$, $\Lambda = 9.7313$, and the conditions in Theorem 1 can be satisfied.

The work and rest intervals of controller (25) are shown in Figure 3. Under control scheme (25), the state and error trajectories are plotted in Figures 4 and 5. From Figure 4, it can be seen that the state trajectories can achieve a certain consistent behavior. As shown in Figure 5, the synchronization errors converge to zero with $T^{\diamond} = 6.0019$ s under controller (25), demonstrating the FTS of system (23) can be realized.

Figure 6 depicts the evolution of control scheme (25). From Figures 4–6, it shows that the designed approach proposed in this paper is efficient.

To further evaluate the effectiveness of the proposed control method under different initial conditions and fractional orders, three simulation cases are considered. The network parameters, controller gains, and aperiodic intermittent control schedule are consistent across the three cases, while the initial conditions or the fractional order are varied. The corresponding comparisons of the function $V(t)$ are presented in Figure 7, where Figure 7a illustrates the results under different initial conditions with $\beta = 0.98$, and Figure 7b shows the results under different fractional orders with identical initial conditions.

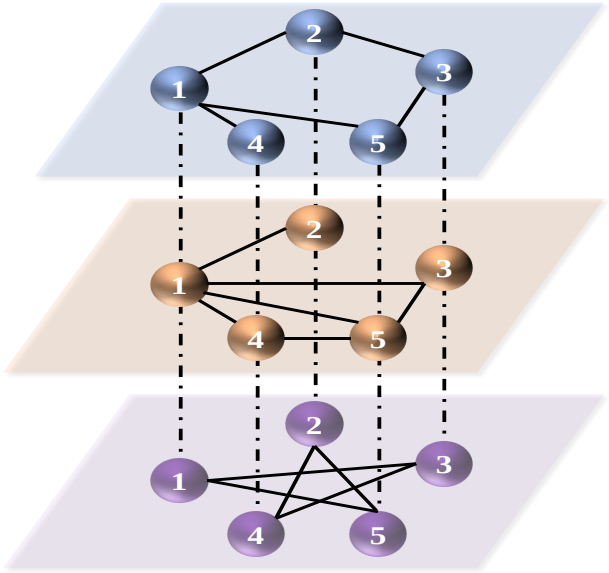


Figure 1. The topological structure of system (23). The first, second, and third layers are represented by blue, orange, and purple nodes, respectively.

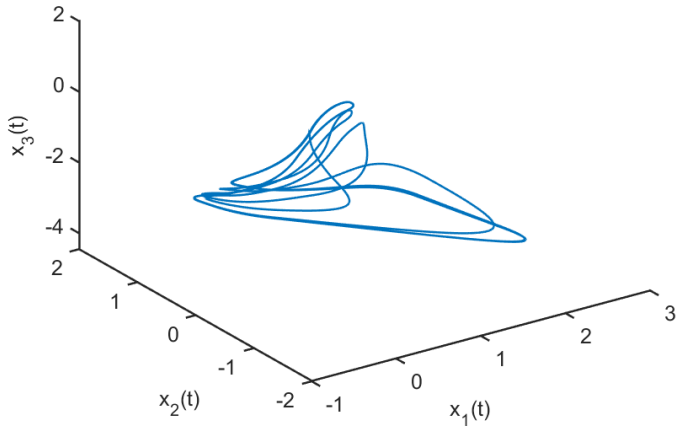


Figure 2. The chaotic phenomenon of system (24).

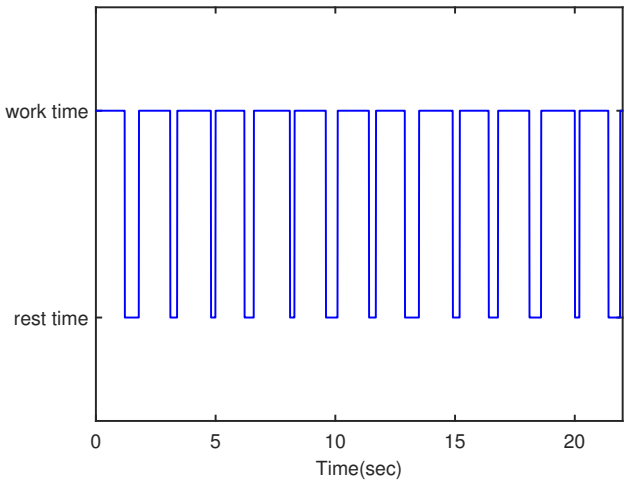


Figure 3. Work and rest time of aperiodic intermittent controller (25).

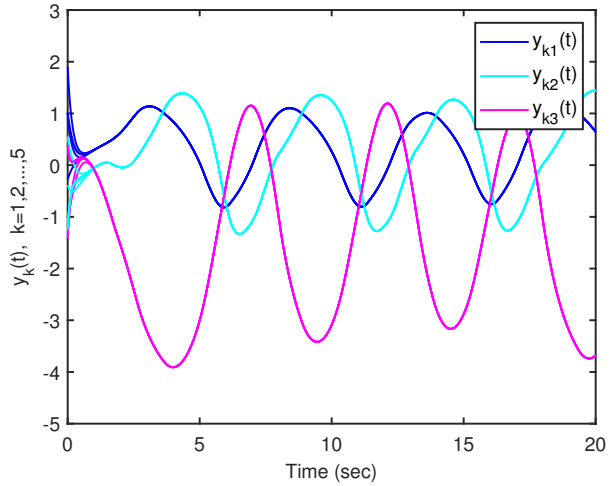


Figure 4. The state trajectories of system (23) under controller (25).

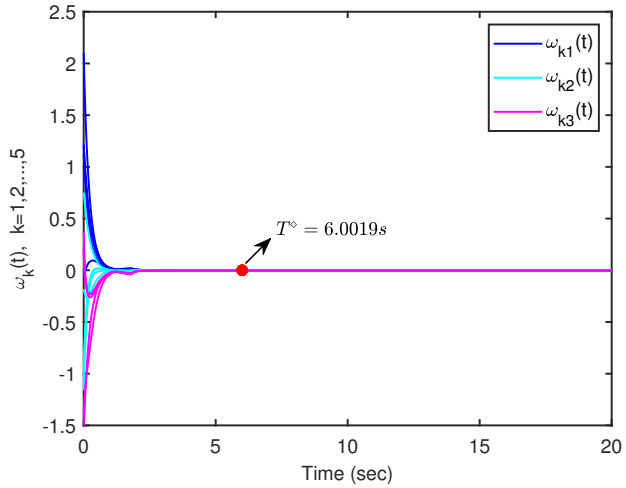


Figure 5. The evolution of the synchronization errors under controller (25).

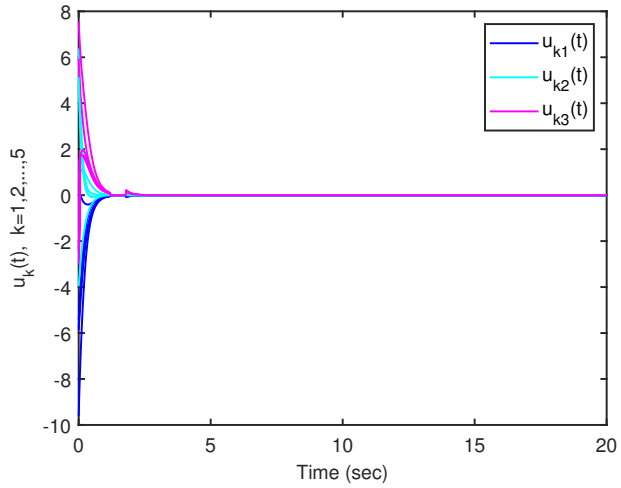


Figure 6. Evolution of controller (25).

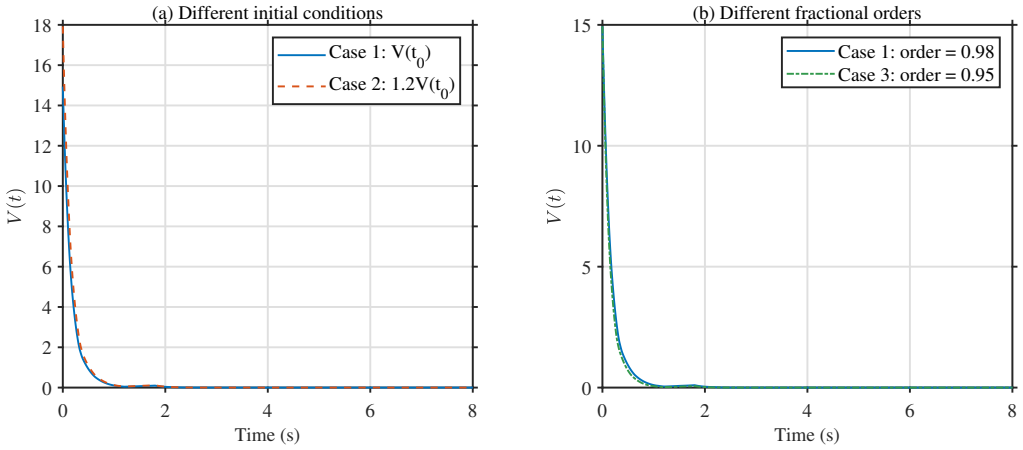


Figure 7. Comparison of the function $V(t)$: (**a**) different initial conditions with $\beta = 0.98$; (**b**) different fractional orders with identical initial conditions.

- Case 1: The fractional order is $\beta = 0.98$, and the initial conditions are those specified above.
- Case 2: The fractional order remains $\beta = 0.98$ with $1.2V(t_0)$. The initial conditions of system (24) remain unchanged.
- Case 3: The fractional order is changed to $\beta = 0.95$, while the initial conditions remain the same as in Case 1.

5. Conclusions

This paper is concerned with the FTS problem of discontinuous FMLCNNs via aperiodic intermittent control. Above all, a novel piecewise fractional-order differential inequality is established over the control and rest intervals, which provides an effective tool for the FTS analysis of discontinuous FMLCNNs. Then, under the Filippov differential inclusion framework, an aperiodic intermittent controller has been designed to deal with the nonsmooth neural dynamics. Furthermore, FTS conditions are derived based on the proposed piecewise fractional-order differential inequality and Lyapunov analysis. Finally, a numerical example is presented to show the validity of theoretical results. It should be noted that time delays have not been considered in this paper, since the proposed analytical method and control strategy are not directly applicable to fractional-order time-delay systems. Therefore, extending the present results to FMLCNNs with time delays will be considered in future works.

Author Contributions: Conceptualization, B.Z.; methodology, B.Z.; software, Y.X.; validation, Y.X.; formal analysis, Y.X.; writing—original draft preparation, B.Z.; writing—review and editing, W.D.; supervision, W.D.; funding acquisition, W.D. All authors have read and agreed to the published version of the manuscript.

Funding: This work was supported by the National Key Research and Development Program of China under Grant 2022YFB3304700, the Science Fund for Distinguished Young Scholars of Jiangsu Province under Grant BK20240102, the National Natural Science Foundation of China under Grants 62373361 and 62503480, the China Postdoctoral Science Foundation under Grant 2025M783157, and the Fundamental Research Funds for the Central Universities under Grant 2025QN1070 (*Corresponding author: Wei Dai).*

Data Availability Statement: The original contributions presented in this study are included in the article. Further inquiries can be directed to the corresponding author.

Conflicts of Interest: The authors declare no conflicts of interest.

References

1. Shang, C.; Sun, K.; Wang, H.; He, S. Spatial patterns and chimera states in discrete memristor coupled neural networks. *Nonlinear Dyn.* **2023**, *111*, 20347–20360.
2. Wang, M.; Zhu, S.; Luo, W.; Zhang, Z. Finite-/Fixed-Time Synchronization of Coupled Memristive Neural Networks With Actuator Nonlinearity and Applications in Secure Communication. *IEEE Trans. Circuits Syst. I Regul. Pap.* **2025**, *72*, 4334–4345.
3. Kumar, V.; Prasad, U.; Mohanty, S.R. Entirely Coupled Recurrent Neural Network-Based Backstepping Control for Global Stability of Power System Networks. *IEEE Trans. Autom. Sci. Eng.* **2024**, *21*, 1647–1660.
4. Hui, Y.; Chen, S.; Liu, X.; Meng, W. Physically Consistent Modeling for Multi-Layer Reconfigurable Intelligent Surface-Based Multi-User Communications. *IEEE Trans. Wirel. Commun.* **2026**, *25*, 6004–6019.
5. Li, J.; Li, Z.; Qi, X. A review of multilayer networks-based interregional transportation networks analysis. *Chaos Solitons Fractals* **2025**, *192*, 115993.
6. Liu, L.; Liang, Y.; Feng, J.; Pei, Q.; Su, S.; Qu, Y.; Wu, C. Intelligence-Empowered Multi-Tier Cross-Domain Collaborative Computing for Scalable AAV-Enabled Low-Altitude Economy Networking. *IEEE Wirel. Commun.* **2026**, *33*, 29–35.
7. He, S.; Vignesh, D.; Rondoni, L.; Banerjee, S. Chaos and multi-layer attractors in asymmetric neural networks coupled with discrete fractional memristor. *Neural Netw.* **2023**, *167*, 572–587.
8. An, X.; Jiang, L.; Zhang, J. Synchronization behavior and energy evolution in physical neuron and network. *Nonlinear Dyn.* **2024**, *112*, 16389–16407.
9. Xia, M.; Wang, J.; Liu, N.; Xie, Y.; Yue, Z.; Shi, C.; Chen, W.; Mou, X. Multimodal Spatiotemporal Feature-Based Human Motion Pattern Recognition With CNN-Transformer-Attention Framework. *IEEE Internet Things J.* **2025**, *12*, 43883–43895.
10. Cao, Y.; Long, T.; Sun, J.; Wang, Z.; Xu, G. Comparison of Distributed Task Allocation Algorithms Considering Non-Ideal Communication Factors for Multi-UAV Collaborative Visit Missions. *IEEE Robot. Autom. Lett.* **2025**, *10*, 1928–1935.
11. Ren, Y.; Jiang, H.; Hu, C.; Hu, L.; Li, J. Synchronization of quaternion-valued multi-layer coupled networks: An adaptive activation-time-based event-triggered scheme. *Inf. Sci.* **2025**, *706*, 121999.
12. Ding, S.; Hu, L.; Rong, N. Synchronization in Multi-Layer Networks with Aperiodically Intermittent Adaptive Coupling. *IEEE Trans. Consum. Electron.* **2026**, *72*, 1793–1801.
13. Xu, D.; Song, S.; Ahn, C.K.; Su, H. An Intermittent Volatile Event-Triggered Synchronization Approach for Multi-Layer Networks With Noise Coupling Under an Almost Sure Framework. *IEEE Trans. Autom. Sci. Eng.* **2025**, *22*, 11150–11162.
14. Podlubny, I. *Fractional Differential Equations*; Mathematics in Science and Engineering; Elsevier: Amsterdam, The Netherlands, 1999.
15. Pavithra1, G.; Dharani1, S.; Sivakumar, M. Finite-time synchronization of fractional-order fuzzy cellular neural networks with mixed delays and interactions via quantized memory sampled-data control. *Int. J. Dyn. Control* **2026**, *14*, 356.
16. Pavithra1, G.; Dharani1, S.; Sivakumar, M. Synchronization Analysis of Fractional-Order Competitive Neural Networks with Additive Time Varying Delay via Quantized Sampled Data Control and Its Application to Image Encryption. *Complex Anal. Oper. Theory* **2026**, *20*, 174.
17. Zhang, Y.; Wang, F.; Wei, Y.; Zhang, C. Exponential outer quasi-synchronization of delayed fractional fuzzy reaction-diffusion coupled cellular neural networks via impulsive control. *J. Appl. Math. Comput.* **2026**, *72*, 29.
18. Zheng, B.; Wang, Z. Mittag-Leffler synchronization of fractional-order coupled neural networks with mixed delays. *Appl. Math. Comput.* **2022**, *430*, 127303.

19. Zhang, W.; Zhu, H.; Che, H.; Wang, X.; Li, H.; Li, H. Bipartite Synchronization of Fractional-Order Multi-Layer Signed Network With a Non-Autonomous Leader. *IEEE Trans. Circuits Syst. I Regul. Pap.* **2025**, *72*, 8396–8407.
20. Wei, C.; Wang, X.; Hui, M.; Zeng, Z. Quasi-Synchronization of Fractional Multi weighted Coupled Neural Networks via Aperiodic Intermittent Control. *IEEE Trans. Cybern.* **2024**, *54*, 1671–1684.
21. Xu, Y.; Zhen, S.; Xie, X. Security Quasi-Synchronization Control of Fractional-Order Fuzzy Multiplex Networks With Short Memory Windows. *IEEE Trans. Emerg. Top. Comput. Intell.* **2026**, *10*, 3482–3494.
22. Li, Y.N.; Wang, J.L.; Ren, S.Y.; Huang, T. Bipartite and H_∞ bipartite synchronization for multiweighted coupled fractional-order delayed reaction-diffusion neural networks. *Neural Netw.* **2026**, *201*, 108863.
23. Wang, X.; Gu, H.; Jinhu, L. Asymptotic and finite-time synchronization for fractional-order multiplex neural networks with multiple delays. *Sci. China Technol. Sci.* **2025**, *68*, 1620401.
24. Qiu, P.; Tan, M.; Luo, M.; Wu, K. Practical finite-time bipartite synchronization for fractional-order T–S fuzzy multilayer signed networks via dynamic event-triggered hybrid impulsive control. *Math. Comput. Simul.* **2026**, *242*, 297–322.
25. Qiu, P.; Tan, M. Finite-Time Intra-Layer and Inter-Layer Synchronization of Fractional-Order Multi-Layer Networks With Time-Varying Delays. *Math. Methods Appl. Sci.* **2026**, *49*, 10108–10132.
26. Mei, Y.; Wang, B.; Jian, J.; Wu, K. Finite-time synchronization of fractional-order competitive memristive fuzzy neural networks with time-varying delays via aperiodic intermittent quantized control. *J. Frankl. Inst.* **2026**, *363*.
27. Zhang, W.; Zhu, H.; Wen, S.; Huang, T. Finite-Time Bipartite Tracking Consensus of Fractional-Order Multi-Layer Signed Networks by Aperiodically Intermittent Control. *IEEE Trans. Circuits Syst. II Express Briefs* **2024**, *71*, 3061–3065.
28. Filippov, A.F. *Differential Equations with Discontinuous Right-Hand Side*; Kluwer Academic Publishers: Dordrecht, The Netherlands, 1964.
29. Cai, S.; Hou, M. Quasi-synchronization of fractional-order heterogeneous dynamical networks via aperiodic intermittent pinning control. *Chaos Solitons Fractals* **2021**, *146*, 110901.
30. Alsina, C.; Tomás, M.S. A Geometrical Proof of a New Inequality for the Gamma Function. *J. Inequalities Pure Appl. Math.* **2013**, *6*, 48.
31. Yang, D.; Sun, N.; Ma, T. Stability analysis for nonlinear fractional-order systems based on comparison principle. *Nonlinear Dyn.* **2014**, *75*, 387–402.
32. Yang, S.; Yu, J.; Hu, C.; Jiang, H. Finite-Time Synchronization of Memristive Neural Networks With Fractional-Order. *IEEE Trans. Syst. Man Cybern. Syst.* **2021**, *51*, 3739–3750.
33. Hou, T.; Yu, J.; Hu, C.; Jiang, H. Finite-Time Synchronization of Fractional-Order Complex-Variable Dynamic Networks. *IEEE Trans. Syst. Man Cybern. Syst.* **2021**, *51*, 4297–4307.
34. Clarke, F.H.; Ledyaev, Y.S.; Stern, R.J.; Wolenski, P.R. *Nonsmooth Analysis and Control Theory*; Springer: Berlin/Heidelberg, Germany, 2009.
35. Wang, Z.; Zheng, B. Saturation Function-Based Finite-Time Synchronization Control for Fractional-Order Coupled Neural Networks. *IEEE Trans. Autom. Sci. Eng.* **2025**, *22*, 16658–16667.
36. Luo, D.; Wang, C.; Liang, J.; Deng, Q. Memristor coupled fractional-order Hopfield neural network composed by heterogeneous neurons and its FPGA implementation. *Nonlinear Dyn.* **2025**, *113*, 29983–29998.

Disclaimer/Publisher's Note: The statements, opinions and data contained in all publications are solely those of the individual author(s) and contributor(s) and not of MDPI and/or the editor(s). MDPI and/or the editor(s) disclaim responsibility for any injury to people or property resulting from any ideas, methods, instructions or products referred to in the content.